Appl. Phys. B (2012) 109:113–119
DOI 10.1007/s00340-012-5191-6

Applied Physics B
Lasers and Optics

Study of THz-wave-induced photoluminescence quenching in GaAs and CdTe

Zheng Chu · Jinsong Liu · Jingle Liu

Received: 30 November 2011 / Revised: 5 June 2012 / Published online: 23 September 2012
© Springer-Verlag 2012

Abstract A novel model of ultrafast interaction between THz pulse and carriers is built to study the THz-wave-induced quenching of femtosecond-laser-excited photoluminescence in CdTe and GaAs. Photoluminescence quenching is due to the nonequilibrium intervalley phonons induced by the THz field and subsequent decrease of the recombination efficiency of the electron–hole pairs. And the PLQ versus laser intensity experimental result agrees with the analysis.

1 Introduction

The dynamics of photoluminescence (PL) quenching (PLQ) can reveal rich information of carrier transport, scattering, and lattice vibration in semiconductors [1–8]. As a result, the study of PLQ has attracted considerable attention during the past decades due to its potential applications in optoelectrons and photonics, such as PL in quantum wells quenched by far-infrared radiation [1] or by dc electric field [2], and PL in disordered semiconductors quenched by temperature [3]. Recently, an experiment of PLQ in bulk semiconductors induced by ultrashort THz pulse was reported [4] where an 800 nm femtosecond (fs) pulse was used to excite CdTe and GaAs and PL near bandgap was measured. As a single-cycle THz pulse was illuminated on the samples simultaneously, the amplitude of the time-integrated PL was found to be decreased.

When femtosecond (fs) laser pulses irradiate on semiconductors, the electron will be excited from the valence band to the conduction band, creating electron–hole pairs. The PL emission comes from the radiative recombination between the electron near the bottom of conduction band and the holes at top of the valence band. The incident THz waves "accelerate" or "heat" electrons [5] and promote them to high-energy states in the conduction band. The high-energy carriers can induce nonequilibrium phonons which increase the nonradiative centers by phonon–defect coupling [9–11]. Subsequently, the intensity of the radiative recombination of the electron–hole pairs decreases. Finally, we can observe THz-induced PLQ. Based on the viewpoint mentioned above, we combine ensemble Monte Carlo method [8, 12] with nonlinear photon excitation model [13] to describe the transition in bulk semiconductors. Via this model, we systematically investigate the dynamics and THz intensity dependence of quantum efficiency in GaAs and CdTe. Using an experimental setup similar to that in [4], we measure the laser intensity dependence of PLQ in CdTe. The measured results agree well with the calculated ones. Our study on the THz-pulse-modulated PL could potentially lead to applications of a noninvasive ultrafast modulator of light-emitting and THz electro-absorption modulation [14–17].

Z. Chu · J. Liu (✉)
Wuhan National Laboratory for Optoelectronics, School of Optoelectronic Science and Engineering, Huazhong University of Science and Technology, Wuhan 430074, China
e-mail: jsliu4508@vip.sina.com

J. Liu
Department of Physics, Applied Physics and Astronomy, Center for Terahertz Research, Rensselaer Polytechnic Institute, Troy, NY 12180, USA

2 Physical mechanism and model

Scattering of electrons between the different valleys of the conduction band in a semiconductor plays an important role in high field transport process. Under a strong THz

field (peak value is above 100 kV/cm), both intrinsic and photo-induced carriers may absorb/emit phonons through intervalley scattering and then intervalley phonons become nonequilibrium. These hot phonons usually have large wave vectors which induce vibration of very few atoms, and their energy can be easily coupled by nonradiative centers such as point defects [18–20]. As a result, PL quantum efficiency quenches.

2.1 Monte Carlo simulation of carriers' transport and scattering

THz wave can drive carriers before and during photon excitation. The dynamical evolution of the carrier–phonon system can be described by the coupled Boltzmann equations [8, 21, 22]:

$$\frac{\partial f_k}{\partial t} = \left.\frac{\partial f_k}{\partial t}\right|_g + \left.\frac{\partial f_k}{\partial t}\right|_{c-\mathrm{ph}} + \left.\frac{\partial f_k}{\partial t}\right|_{c-\mathrm{impurity}} + \frac{eE_t(t)}{\hbar}\nabla_k f_k, \quad (1)$$

$$\frac{\partial N_q}{\partial t} = \left.\frac{\partial N_q}{\partial t}\right|_{c-\mathrm{ph}} + \left.\frac{\partial N_q}{\partial t}\right|_{\mathrm{ph-ph}} + \left.\frac{\partial N_q}{\partial t}\right|_{\mathrm{ph-nr}}, \quad (2)$$

where f_k and N_q are the electron and the phonon distribution function, respectively. $\partial f_k/\partial t|_g$ stands for photo induced carriers generation and $\partial f_k/\partial t|_{c-\mathrm{ph}}$ and $\partial f_k/\partial t|_{c-\mathrm{impurity}}$ are carrier–phonon and carrier–impurity interaction rates, respectively. The THz-filed-driven process is described by $eE_t(t)\nabla_k f_k/\hbar$, in which e is the unit charge with its sign ($e < 0$ for electrons and $e > 0$ for holes), and $\hbar$ is the Planck constant divided by 2π. Particularly, E_t is equal to $(2Y_0E_{\mathrm{THz}} - Jd)/(Y_0 + Y_s)$, and is the THz field transmitted through the thin semiconductor film [23]. Here E_{THz} is the incident THz field, d is the laser penetration depth (1 μm for the 800-nm laser pulse), and Y_0 and Y_s are the free-space and sample admittances, respectively. The current density J is $(ne^2\tau/m)E_t$. Here n is the carrier density, τ denotes mean free time between ionic collisions and m is carrier mass. $\partial N_q/\partial t|_{\mathrm{ph-ph}}$ and $\partial N_q/\partial t|_{\mathrm{ph-nr}}$ are the phonon decay rates for phonon–phonon and phonon-nonradiative center interactions, respectively. The acoustical phonon, polar-LO phonon and intervalley phonon are taken into consideration. The holes effect is neglected due to the high effective mass. Equation (1) is usually calculated by using ensemble Monte Carlo simulation (EMC) [11]. In order to calculate nonequilibrium phonons exactly, we use fictitious scattering method [24, 25] to obtain the carrier–phonon scattering rates.

In Eq. (2), $\partial N_q/\partial t|_{c-\mathrm{ph}}$ can be written as $A\Delta h_q$ [21]. Δh_q is changed at each phonon scattering time, A is a normalized factor, when THz field is applied in one direction (we can assume that it is Z direction) [26],

$$A = \pm\frac{8\pi^2}{2q_T\Delta q_T\Delta q_Z + \Delta q_T^2\Delta q_Z}\frac{n}{N_e}, \quad (3)$$

where sign '+' corresponds to the emission and '−' to the absorption of the phonon with the wave vector $q = \{q_Z, q_T\}$, q_Z is the phonon wave vector along Z direction, $q_T = \sqrt{q_X^2 + q_Y^2}$, Δq_T and Δq_Z are the steps of the q-grid and N_e is the number of simulated particles.

2.2 Theoretical model for laser excitation and PL emitting

Since the focal spot diameter of the 0.15 μJ optical pulse is 0.05 mm, i.e., the pump pulse fluence is higher than 5 mJ/cm^2, the two-photon absorption (TPA) should become prominent at such excitation levels. The propagation of the optical pump pulse in the direction perpendicular to the surface of the semiconductors is then described by the following pair of differential equations [13, 27]:

$$\frac{\partial I(z,t)}{\partial z} = -\alpha I(z,t) - \beta I^2(z,t) - \frac{1}{v_g}\frac{\partial I(z,t)}{\partial t}, \quad (4a)$$

$$\frac{\partial N_{\mathrm{SPA}}(z,t)}{\partial t} = \frac{\alpha I(z,t)}{\hbar\omega}, \quad (4b)$$

$$\frac{\partial N_{\mathrm{TPA}}(z,t)}{\partial t} = \frac{\beta I^2(z,t)}{2\hbar\omega}, \quad (4c)$$

where $I(z,t)$ is the pump beam intensity, $N_{\mathrm{SPA}}(z,t)$ and $N_{\mathrm{TPA}}(z,t)$ are the density of single-photon absorption (SPA) and TPA excited particles, respectively, ω is the angular frequency of the pump pulse, $\alpha = 1/d$ is the linear absorption coefficient at 800 nm, $\beta = \beta_{[100]} \propto \mathrm{Im}\chi^3_{1111}$ is TPA coefficient and χ^3_{1111} is the third-order nonlinear tensor of the susceptibility. v_g is the beam's group velocity. $N_{\mathrm{SPA}}(z,t)$ and $N_{\mathrm{TPA}}(z,t)$ should be distinguished in the Monte Carlo simulation since the electrons generated from SPA and TPA, respectively, have excess energies. The mean concentration in the photo-excited region can be described as $n(t) = \int_d \mathrm{d}z \frac{N_{\mathrm{SPA}}(z,t)+N_{\mathrm{TPA}}(z,t)}{d}$.

After photo-excitation, the time dependence of the excess carrier concentration is governed by the rate equation [28]:

$$\frac{\mathrm{d}n(t)}{\mathrm{d}t} = -\frac{n(t)}{\tau_{\mathrm{eff}}(t)}, \quad (5)$$

where the effective carriers' lifetime $\tau_{\mathrm{eff}}(t) = \frac{\tau_r(t)\tau_{\mathrm{nr}}}{\tau_r(t)+\tau_{\mathrm{nr}}}$ [29]. The radiative lifetime $\tau_r(t) = 1/Bn(t)$, B (10^{-9} cm^3 s^{-1} in CdTe) is the radiative rate constant [27]. Since large quantities of hot optical phonons will likely lead to generation of new defects [10, 11], the nonradiative lifetime is assumed to be

$\tau_{nr} = 1/C\int_{T_p} dt N_{qne}(t)/\tau_{ne}$, C is the nonradiative rate constant of defects, we favor a value of $C = 2 \times 10^{-7}$ cm^3 s^{-1}. T_p is the pump duration, τ_{ne} is the lifetime of nonequilibrium intervalley phonons. $N_{qne}(t) = \sum_q (N(q,t) - N_0)D(q)$ is the total number of out of equilibrium intervalley phonons [30], $N_0 = 1/[\exp(h\omega_q/k_B T) - 1]$, $h\omega_q$ is intervalley phonon energy. Refer to Eq. (3), phonon density of state $D(q) = 2q_T\Delta q_T\Delta q_Z + \Delta q_T^2\Delta q_Z$. Since the decay nonradiative centers are much longer than τ_{eff}, τ_{nr} it is usually treated as time-independent when phonons return to equilibrium.

As we know, PL effect is the consequence of radiative recombination. The time-integrated PL is determined by the total number of radiative carriers $I_{PL} \propto N_r$,

$$N_r = V\int_{\infty} dt \frac{n(t)}{\tau_r(t)} \tag{6}$$

V is the size of photon-excited region. After derivation from Eqs. (5) and (6) one can have $N_r$expression as

$$I_{PL} \propto N_r = V\int_0^{\infty} dt\left\{Bn_0 n(t) - \int_0^t d\tau n(\tau)\left(\frac{1}{\tau_{nr}} + Bn(\tau)\right)\right\} \tag{7}$$

n_0 is the carrier concentration at the end of the pump pulse $t = 0$.

In summary, the simulation procedure for the isotropic electron and phonon distributions is as the following:

At first, initialization of all the parameters is necessary. In each time step,

1. Calculation of the carrier density $n(t)$ from Eqs. (4a, 4b, 4c) if $I(z,t) > 0$.
2. Calculation of THz field E_t.
3. EMC calculation from Eqs. (1) and (2).
4. Refresh the τ mean free flight time and nonequilibrium phonon density $n_{qne}(t)$.
5. If optical excitation is over, calculate I_{PL} from Eqs. (5) and (6).

By using the model above, we calculate the PLQ and THz intensity dependence of PLQ in CdTe and GaAs. These calculated results are compared with previous measurements [4]. Furthermore, we experimentally and theoretically investigate the laser intensity dependence of PLQ in CdTe. The parameters used for calculation are listed. Figure 1 is the scattering rates versus energy in GaAs (a) and CdTe (b) at room temperature in the Γ valley.

3 Major mechanisms in THz-induced PLQ process

3.1 Reflection after photo-excitation

The high concentration of photo-excited carriers results in a very high THz reflectivity coefficient of the sample interface, thus decreasing the coupling of THz field to the bulk of the carriers.

3.2 Phonons generation via relaxation of intrinsic carriers

The n-doping values of GaAs and CdTe are 1×10^{16}–3×10^{16} cm^{-3} (2×10^{16} cm^{-3} in calculation) and 8×10^{16}–3×10^{17} cm^{-3} (2×10^{17} cm^{-3} in calculation). Though the doping values are much lower than laser excitation density (about 2×10^{19}/cm^3), they play important roles at the initial and mid stage of excitation. Figure 2 is the intervalley phonon distributions induced by intrinsic carriers as a function of time delay t_d (<0 means the peak of THz wave is behind optical pulse excitation) between THz wave and laser pulse. The central wave vectors of GaAs and CdTe intervalley phonon are about 10^7 and 2×10^7/cm, respectively. Their magnitudes are higher than that of nonequilibrium LO phonon and they are more easily absorbed by nonradiative centers.

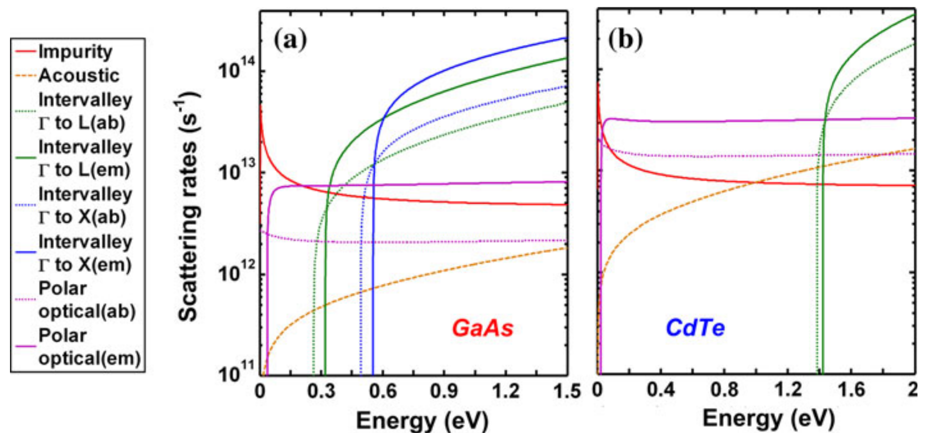

Fig. 1 Scattering rates versus energy in GaAs (**a**) and CdTe (**b**) at room temperature in the Γ valley

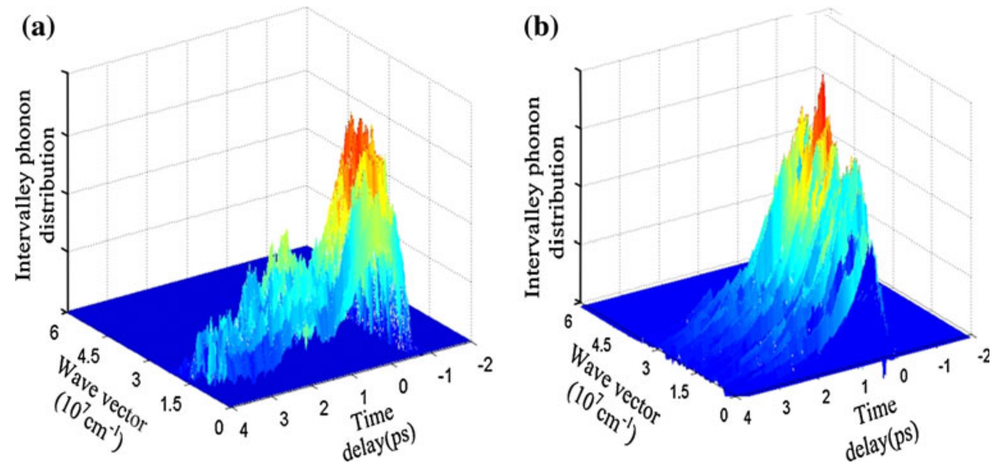

Fig. 2 The calculated the intervalley phonon distribution generated from intrinsic carriers transition in **a** GaAs and **b** CdTe in a strong THz field (100 kV/cm)

3.3 Phonons generation via relaxation of photo-excited carriers

The orange curves in Fig. 3 are the evolution of the mean energy of photo-excited carriers at $t_d = 0$. The Γ–L separation in GaAs is only 0.29 eV, thus the kinetic energies of photo-induced carriers are sufficient for the intervalley transition. And the hot phonons in GaAs can be generated via the intervalley transition of photo-induced carriers. The blue curve in Fig. 3a shows the generation and decay of these phonons. On the other hand, both the Γ–L separation (1.4 eV) and effective electron mass (0.11 m_0) in CdTe are much larger than that in GaAs. Even if the THz field is as strong as 100 kV/cm, as Fig. 3b shows, the photo-excited carriers cannot be accelerated to the necessary energy level. As a result, they will not change the intervalley phonon occupation.

4 Results and discussion

Since the intervalley phonon distribution is determined, we can calculate the time-integral PL intensity as a function of time delay t_d via Eq. (7) as shown in Fig. 4 in which the THz time-domain waveform measured by electro-optic sampling is plotted together. The shapes of the calculated curves agree well with those of the measured ones (see Fig. 3 in [4]). The calculated curves show that the PL drops as the laser pulse starts to overlap with THz pulse, and recovers back to the level without THz radiation when t_d increases from 0. There are two key time delays which proof of the accuracy of this theoretical model: (1) $t_d = -1$ ps (when the peak of THz wave was 1 ps behind optical pulse excitation). The high concentration of carriers results in a very high THz reflectivity. Both calculation and experimental result [4] show that PLQ ratio should be zero when $t_d = -1$ ps; (2) $t_d = 1$ ps. The sample of GaAs exhibits a faster recovery than that of CdTe. Since the strong THz field can drive the photo-induced carriers to Γ−L separation energy before the high THz interface reflection forms in GaAs, the energies of photo-induced carriers are governed by the transient THz wave in the optical excitation duration. As a result, the PL curve is more sensitive to the transient THz intensity; In CdTe, the photo-induced carriers have not enough energy to generate phonons via intervalley transition. As a result, the PLQ effect in CdTe only results from the intrinsic carriers which is more sensitive to time-integrated THz intensity. Therefore, PLQ trace of CdTe has a boarder temporal quenching window than that of GaAs. The calculated PLQ ratios that are about 1 and 10 % in CdTe and GaAs, respectively, at t_d is 1 ps also agree well with those of the previous measurement [4].

In order to further verify that PLQ of CdTe is only induced by the nonequilibrium intervalley phonons from intrinsic carriers, the laser intensity dependence of the PLQ ratio is experimentally investigated and compared with the calculation using the model above. Here PLQ ratio = 100 % − $I_{PL}(E_{THz} \neq 0)/I_{PL}(E_{THz} = 0)$. We expected that the PLQ ratio should monotonically decrease with laser intensity. The physical mechanism is that when the laser intensity becomes stronger, the number of the corresponding photo-induced carriers becomes larger. If those carriers make no contribution to hot intervalley phonons, they will reduce the ratio between nonradiative and radiative recombination rates. Then the PLQ ratio will reduce. In theoretical expression, when excited carriers density $n(\tau)$ grows, the damping term $1/\tau_{nr} + Bn(\tau)$ in Eq. (7) becomes τ_{nr}-independent when $Bn(\tau) \gg 1/\tau_{nr}$ (Table 1).

In the experiment, the PL emitted from CdTe is filtered by a narrow line interference filter (center transmission wavelength ~840 nm, and bandwidth ~10 nm) and then collected by a photomultiplier tube. The time delay

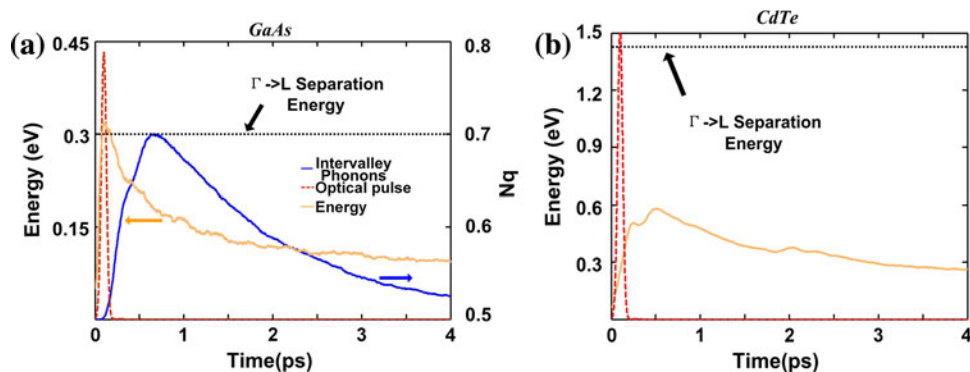

Fig. 3 The evolution of mean carrier energy (*orange line*) and intervalley phonons occupation (*blue line*) PL at $t_d = 0$ in comparison with the time-domain waveform of the optical pulse (*dashed red line*)

Table 1 The parameters used for calculation

Parameters	GaAs	CdTe	Unit
Bandgap at 300 K			
$E_{hh\text{-}\Gamma}$	1.42	1.47	eV
$E_{\Gamma L}$ ($E_{\Gamma X}$)	0.29 (0.52)	1.4	eV
Effective mass			
m_Γ	0.067	0.11	m_0
m_L (m_X)	0.22 (0.58)	0.5	m_0
Deformation potential			
$D_{\Gamma L}$ (D_{LX})	10 (5)	10	eV/Å
LO phonon energy	35	21	meV
Intervalley phonon energy	27.8	19	eV
Static dielectric function ε_0	12.9	10.6	
High-frequency dielectric function (ε_∞)	10.92	7.13	
Penetration depth	1	1	μm
TPA coefficient	15	170	cm/GW

between the THz pulse and laser pulse is fixed at timing where maximal quenching occurs. The diameter of the THz beam and laser beam on the CdTe sample are about 500 and 50 μm, respectively. The peak THz intensity is fixed at 13 MW/cm^2. The measured data (circles) and the calculated curve (solid curve) are shown in Fig. 5. As can be seen, PLQ ratio reaches to almost zero at high laser intensity. The experiment agrees well with the expectation. It should be noted that some other mechanisms can also affect PLQ ratio decrease: (1) the high THz reflection reduces PLQ ratio. The pink dots curves are the calculated PLQ ratios when the THz reflection change is not taken into consideration. A deviation occurs when the laser intensity reaches 10 GW/cm^2. Under such laser irradiation, the excited carrier's density is 10^{19}/cm^3 which is the threshold density of high THz reflectivity; (2) TPA carriers have much higher excess energies than SPA carriers. They can induce hot phonon markedly without the assist of THz wave, thus reduce the THz modulation efficiency. The dashed green line shows that the error will increase if TPA effect is neglected.

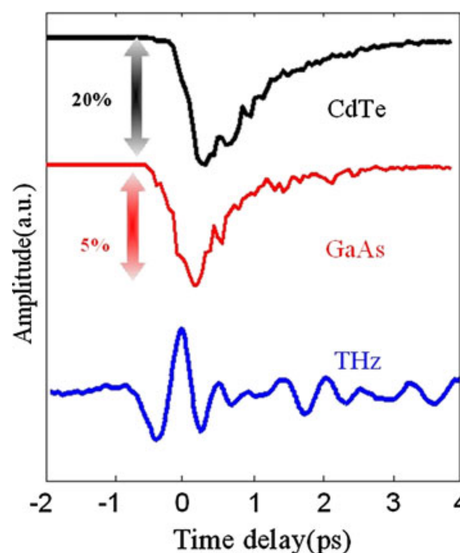

Fig. 4 The calculated PL as a function of time delays between THz and optical pulse in CdTe at 831 nm (*top*) and in GaAs at 854 nm (*middle*) in comparison with the time-domain waveform of a THz pulse (*bottom*)

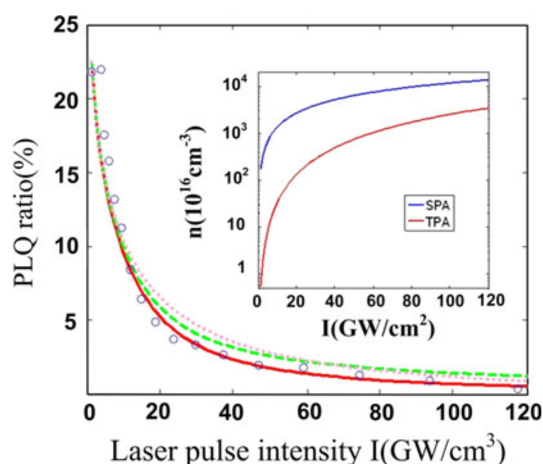

Fig. 5 The measured and calculated curves for the laser pulse energy dependence of PLQ ratio in CdTe. *Blue circles* are experimental result and *red solid line* is calculation of PL quenching ratio. The *green dashed and pink dot lines* are the calculated results neglecting TPA and surface reflectivity of THz, respectively. *Inset* Density of SPA and TPA carriers versus the laser intensity

PLQ ratio in GaAs is relatively small (only 5 % under the THz-pulse irradiation of 100 kV/cm peak field) providing limited study range. PLQ effect in GaAs is more complex in high pump intensity since photon-excited carriers also contribution to the intervalley phonon generation. In addition, PLQ is not found in ZnTe($E_g = 2.23$ eV), $Zn_{1-x}Cd_xTe$ ($E_g > 1.65$ eV) or GaP($E_g = 2.26$ eV) [4]. Intervalley scatterings occur without THz wave because of high excess electron energy (3.1 eV $- E_g$) after two-photon absorption in these samples. Thus, if the optical photo energies are adapted to the bandgaps of these semiconductors, PLQ might be observed in these materials.

5 Conclusion

In conclusion, we combine ensemble Monte Carlo method with underlying photon excitation model to describe PLQ in bulk semiconductors induced by intense THz pulses. The PLQ in GaAs results from the photo-excited and intrinsic carriers, whereas the PLQ in CdTe is determined only by the intrinsic carriers. This work provides an effective approach to study PLQ induced by electromagnetic wave pulses in bulk semiconductors and can be potentially used for analyzing PLQ in other materials such as quantum wells and other quenching factors such as dc electric filed. Further study includes investigation of other effects such as temperature and excitation wavelength effect on bulk semiconductor PLQ.

Acknowledgments The authors are grateful to X.-C. Zhang for useful discussions of the origin of luminescence. This work is supported by the National Natural Science Foundation of China under grant No. 10974063 and 61177095, Hubei Natural Science Foundation under grant No. 2010CDA001, Ph.D. Programs Foundation of Ministry of Education of China under grant No. 20100142110042, and the Fundamental Research Funds for the Central Universities, HUST: 2010MS041 and 2011TS001.

References

1. S.M. Quinlan, A. Nikroo, M.S. Sherwin, M. Sundaram, A.C. Gossard, Photoluminescence from AlxGa1-xAs/GaAs quantum wells quenched by intense far-infrared radiation. Phys. Rev. B **45**, 9428–9431 (1992). http://prb.aps.org/abstract/PRB/v45/i16/p9428_1
2. O. Rubel, S. D. Baranovskii, K. Hantke, B. Kunert, W.W. Rühle, P. Thomas, K. Volz, W. Stolz, Model of temperature quenching of photoluminescence in disordered semiconductors and comparison to experiment. Phys. Rev. B **73**, 233201 (2006). http://prb.aps.org/abstract/PRB/v73/i23/e233201
3. P.R. Hania, I.G. Scheblykin, Electric field induced quenching of the fluorescence of a conjugated polymer probed at the single molecule level. Chem. Phys. Lett. **414**, 127–131 (2005). http://linkinghub.elsevier.com/retrieve/pii/S0009261405012418
4. J. Liu, G. Kaur, X.-C. Zhang, Photoluminescence quenching dynamics in cadmium telluride and gallium arsenide induced by ultrashort terahertz pulse. Appl. Phys. Lett. **97**, 111103 (2010). http://apl.aip.org/resource/1/applab/v97/i11/p111103_s1
5. J. Shah, B. Deveaud, T.C. Damen, W.T. Tsang, A.C. Gossard, P. Lugli, Determination of intervalley scattering rates in GaAs by subpicosecond luminescence spectroscopy", Phys. Rev. Lett. **59**, 2222–2225 (1987). http://prl.aps.org/abstract/PRL/v59/i19/p2222_1
6. A. Amo, M.D. Martín, L. Viña, A.I. Toropov, K.S. Zhuravlev, Photoluminescence dynamics in GaAs along an optically induced Mott transition. J. Appl. Phys. **101**, 081717 (2007). http://jap.aip.org/resource/1/japiau/v101/i8/p081717_s1
7. A. Othonos, Probing ultrafast carrier and phonon dynamics in semiconductors. J. Appl. Phys. **83**, 1789 (1998). http://jap.aip.org/resource/1/japiau/v83/i4/p1789_s1
8. Z. Chu, J. Liu, K Wang, Coherent detection of THz waves based on THz-induced time-resolved luminescence quenching in bulk gallium arsenide. Opt. Lett. **37**, 1433 (2012). http://www.opticsinfobase.org/ol/abstract.cfm?uri=ol-37-9-1433
9. F. Gao, D.J. Bacon, P.E.J. Flewitt, T.A. Lewis, The effects of electron–phonon coupling on defect production by displacement cascades in alpha-iron. Model. Simul Mater. Sci. Eng. **6**, 543–556 (1998). http://iopscience.iop.org/0965-0393/6/5/003
10. J.H. Leach, et al. Degradation in InAlN/GaN-based heterostructure field effect transistors: Role of hot phonons. Appl. Phys. Lett. **95**, 223504 (2009). http://apl.aip.org/resource/1/applab/v95/i22/p223504_s1
11. H. Morkoç, *Handbook of Nitride Semiconductors and Devices, GaN-based Optical and Electronic Devices*. (Wiley, New York, 2009)
12. C. Jacoboni, L. Reggiani, The Monte Carlo method for the solution of charge transport in semiconductors with applications to covalent materials. Rev. Mod. Phys. **55**, 645–705 (1983). http://rmp.aps.org/abstract/RMP/v55/i3/p645_1
13. F. Kadlec, H. Němec, P, Kužel, Optical two-photon absorption in GaAs measured by optical-pump terahertz-probe spectroscopy. Phys. Rev. B **70**, 125205 (2004). http:/prb.aps.org/abstract/PRB/v70/i12/e125205
14. S. Hughes, D.S. Citrin, Ultrafast heating and switching of a semiconductor optical amplifier using half-cycle terahertz pulses. Phys. Rev. B. **58** R15969 (1998). http:/prb.aps.org/abstract/PRB/v58/i24/pR15969_1

15. H. Hirori, M. Nagai, K. Tanaka, Excitonic interactions with intense terahertz pulses in ZnSe/ZnMgSSe multiple quantum wells. Phys. Rev. B **81**, 081305 (2010). http://prb.aps.org/abstract/PRB/v81/i8/e081305
16. M.C. Hoffmann, B.S. Monozon, D. Livshits, E.U. Rafailov, D. Turchinovich, Terahertz electro-absorption effect enabling femtosecond all-optical switching in semiconductor quantum dots. Appl. Phys. Lett. **97**, 231108 (2010). http://apl.aip.org/resource/1/applab/v97/i23/p231108_s1
17. T. Ogawa, S. Watanabe, N. Minami, and R. Shimano, Room temperature terahertz electro-optic modulation by excitons in carbon nanotubes. Appl. Phys. Lett. **97**, 041111 (2010). http://apl.aip.org/resource/1/applab/v97/i4/p041111_s1
18. P.G. Klemens, Proc. Phys. Soc. Lond. Sect. A **68**, 1113 (1955). http://iopscience.iop.org/0370-1298/68/12/303
19. D.T. Morelli, J.P. Heremans, G.A. Slack, Phys. Rev. B **66**, 195304 (2002). http://prb.aps.org/abstract/PRB/v66/i19/e195304
20. M. Yao, T. Watanabe, P.K. Schelling, P. Keblinski, D.G. Cahill, S.R. Phillpot, J. Appl. Phys. **104**, 024905 (2008). http://jap.aip.org/resource/1/japiau/v104/i2/p024905_s1
21. P. Lugli, P. Bordone, L. Reggiani, M. Rieger, P. Kocevar, S.M. Goodnick, Monte Carlo studies of nonequilibrium phonon effects in polar semiconductors and quantum wells. I. Laser photoexcitation. Phys. Rev. B **39**, 7852(1989). http://prb.aps.org/abstract/PRB/v39/i11/p7852_1
22. C.L. Collins, P.Y. Yu, Nonequilibrium phonon spectroscopy: A new technique for studying intervalley scattering in semiconductors. Phys. Rev. B **27**, 2602 (1983). http://prb.aps.org/abstract/PRB/v27/i4/p2602_1
23. F.H. Su, F. Blanchard, G. Sharma, L. Razzari, A. Ayesheshim, T.L. Cocker, L.V. Titova, T. Ozaki, J.-C. Kieffer, R. Morandotti, M. Reid, F.A. Hegmann, Terahertz pulse induced intervalley scattering in photoexcited GaAs. Opt. Express **17**, 9620–9629 (2009). http://www.opticsinfobase.org/abstract.cfm?URI=oe-17-12-9620
24. R. MickeviEius, A. Reklaitis, Monte Carlo study of nonequilibrium phonon effects in GaAs. Solid State Commun. **64**, 1305 (1987). http://www.sciencedirect.com/science/article/pii/0038109887906302
25. R MickeviEius, A Reklaitis, Hot intervalley phonons in GaAs. J. Phys. Condens. Matter **2** 7883(1990). http://iopscience.iop.org/0953-8984/2/39/002
26. R. MickeviEius, A. Reklaitis, Hot phonon effects on electron high-field transport in GaAs. J. Phys. Condens. Matter **1**, 9401(1989). http://iopscience.iop.org/0953-8984/1/47/010
27. S.J. Bepko, Anisotropy of two-photon absorption in GaAs and CdTe. Phys. Rev. B **12**, 669 (1975). http:/prb.aps.org/abstract/PRB/v12/i2/p669_1
28. M. Balkanski, R.F. Wallis, *Semiconductor Physics and Applications.* (Oxford University Press, Oxford, 2000)
29. R. Cohen, V. Lyahovitskaya, E. Poles, A. Liu, Y. Rosenwaks, Unusually low surface recombination and long bulk lifetime in n-CdTe single crystals. Appl. Phys. Lett. **73**, 1400 (1998). http://apl.aip.org/resource/1/applab/v73/i10/p1400_s1
30. H. Hamzeh, F. Aniel, Monte Carlo study of phonon dynamics in III–V compounds. J. Appl. Phys. **109**, 063511 (2011). http://jap.aip.org/resource/1/japiau/v109/i6/p063511_s1